MODELLING OF FUEL CONSUMPTION AND FUEL COST ANALYSIS FOR VEHICLES COMBINATION INTENDED FOR COMPRESSED NATURAL GAS TRANSPORTATION

Dragan Z. VAŠALIĆ[1*], Ivan S. IVKOVIĆ[2], Snežana M. KAPLANOVIĆ[2], Dejan S. MILIČEVIĆ[1], Dušan M. MLADENOVIĆ[2], Dragan S. SEKULIĆ[2], Edin H. SULJOVRUJIĆ[1]

[1]Institute of Nuclear Sciences "Vinča", National Institute of the Republic of Serbia, University of Belgrade, Belgrade, Serbia
[2]Faculty of Transport and Traffic Engineering, University of Belgrade, Belgrade, Serbia
[*]Corresponding author; e-mail: dragan.vasalic@vin.bg.ac.rs

The paper presents a fuel consumption estimation model for vehicles with different fuel types, diesel and compressed natural gas, whose main activity is the transportation of compressed natural gas. The model combines the effects of operational conditions and technical characteristics of vehicles and bodies on fuel consumption. Its output results are displayed as fuel consumption expressed in kilograms of fuel burned per kilometer traveled, depending on the operational speed and the amount of gas transported. The approach includes the effects of different body types, pressure vessels made of steel and composite materials, and their technical characteristics concerning volumes, pressures, and construction materials on transported amount of gas, vehicle mass utilization, fuel consumption, and fuel costs. Considering that the paper analyzes the fuel consumption of vehicles differing in tractor fuel type and the amount of compressed natural gas transported in different body types, fuel costs were also analyzed. The results show that vehicle combinations with pressure vessels made of composite materials transport an average of 44% more gas and have lower fuel consumption for both fuel types. Fuel costs are 36% lower on average for vehicles powered by compressed natural gas and bodies with pressure vessels made of composite materials.

Keywords*: Fuel consumption, Fuel cost, Mass utilization, Heavy-Duty Vehicles, Dangerous goods, Compressed natural gas, Composite pressure vessels, Steel pressure vessels*

1. Introduction

Over the past few decades, heavy-duty vehicle (HDV) manufacturers have invested considerable funds and engineering resources to improve vehicle efficiency while minimizing environmental impact. These improvements primarily involve technical advancements in vehicle and engine design, using lightweight materials for vehicle and body construction, and adopting alternative fuels, with the primary goals of transporting larger quantities of goods, reducing fuel consumption, and lowering exhaust emissions. Previous research [1-13] in efficiency improvement and estimation of fuel consumption in HDVs generally represents models based on data that include operational conditions and technical characteristics of the vehicle and applied engines. The considered models present the fuel consumption of HDVs from energy, economic, and environmental aspects. Barth et al. [1] developed several models to estimate fuel consumption and exhaust emissions in diesel HDVs based on the Comprehensive Modal Emissions Model (CMEM) and a parameterized physical approach.

These models estimate consumption and emissions using input parameters derived from specific engine characteristics, vehicle properties, and operating conditions. Edwardes et al. [2] presented a model for estimating the fuel consumption of diesel and hybrid buses based on the Virginia Tech Comprehensive Power-Based Fuel Consumption Model (VT-CPFM). This model uses data from bus technical specifications available in databases and dynamometer measurements to estimate consumption. Peng et al. [3] introduced an estimation model based on an Engine-based Correction Model (ECM), using input parameters derived from specific engine characteristics and road conditions. Their results showed that ECM performs better than the Virginia Tech Microscopic (VT-Micro) and CMEM models in estimating the fuel consumption of HDVs. The Motor Vehicle Emission Simulator (MOVES) is another model used to estimate fuel consumption and exhaust emissions at both macro and micro levels. However, its accuracy is generally more reliable at the macro level because the input parameters are tailored to vehicle categories rather than individual vehicles' specific characteristics [4].

Ankur et al. [5] developed a comprehensive model for predicting fuel consumption based on the tank-to-wheel principle for various transport types, including passenger and freight traffic. Their model employs a parameterized physical approach to estimate consumption using input parameters such as statistical data on vehicles, transport, road, and climate conditions from national databases. Dindarloo and Siami-Irdemoosa [6] introduced a model that utilizes partial least squares regression (PLSR) and autoregressive integrated moving average (ARIMA) to estimate fuel consumption for HDVs based on cyclical work activities in mines. By applying these methods and input parameters like payload, loading time, loaded idle time, loaded travel time, empty travel time, and idle time, they predicted the consumption of heavy mining dump trucks. Studies [7-10] developed fuel consumption estimation models for HDVs using techniques such as multiple linear regression, random forest (RF), artificial neural networks (ANN), support vector machines (SVM), decision trees (DT), back-propagation neural networks, and kernel nearest neighbor methods. These techniques predict consumption based on input parameters that describe the technical characteristics of the vehicle, as well as transport, road, and climatic conditions. With these models, it is possible to predict HDV's fuel consumption during work activities in mines and construction sites. Perrotta et al. [11] investigated the effectiveness of ANN, RF, and SVM in estimating fuel consumption of vehicle combinations using vehicle databases and route characteristics. These techniques assist managers in making decisions within fleet management processes. Fang et al. [12] introduced a new model that combines Convolutional Neural Networks (CNN) and Generative Adversarial Networks (GAN) to predict fine-grained fuel consumption for each engine speed and torque combination, using input data on engine characteristics. Kan et al. [13] developed a fuel consumption estimation model for HDVs based on Long Short-Term Memory (LSTM) and ANN techniques, representing fuel consumption as a function of engine power.

Previous research focuses on determining the effects of HDVs usage in road traffic or specific operational conditions, such as mines or construction sites, including impacts resulting from the technical characteristics of vehicles, engines, and operational conditions. The specificities of this research are reflected in the HDVs intended for compressed natural gas (CNG) transportation. It introduces the dependence of the transported quantities of gas on the influence of the chemical characteristics of the gas and temperature conditions during filling, as well as the specifics of the technical characteristics of the vehicle and body type. Road transport of CNG belongs to the system of road transport of dangerous goods (RTDG); it is carried out using special HDVs and bodies, battery bodies (vehicles), and multiple element gas containers (MEGC) [14]. The accelerated development of economic activity and the demand for more significant amounts of gas require new structural solutions of bodies with pressure vessels intended for gas storage and transport. Structural solutions correspond to the requirements arising from the transported goods (gases) and depend on the material of the bodies and pressure vessels, the type of vehicle, the technical limitations of the vehicle in terms of maximum permissible axle loads, etc. Responses to the demand for more significant amounts of gas while preserving economic sustainability, safety, and the environment lead to applying bodies

with pressure vessels made of composite materials [15-18]. Applying new structural solutions for gas transportation also requires the development of performance assessment models in terms of fuel consumption, exhaust emissions, and cost efficiency under different vehicle operating conditions.
Following the previous, the paper aims to develop a model for estimating the fuel consumption of road vehicle combinations used for CNG transport. The model considers different vehicle subsystem variants (primarily fuel type and gas storage method) and their impact on fuel consumption, depending on the operational speed of the route. By determining the direct effects of the application of vehicles and bodies, the model provides fleet owners with reliable data in decision-making procedures regarding selecting new vehicles or converting existing ones, ultimately improving transport efficiency and reducing fuel costs. Accordingly, the initial research hypotheses are:

- Vehicle combinations powered by CNG equipped with composite material pressure vessels achieve lower fuel consumption and fuel costs than diesel vehicles and those with steel pressure vessels.
- Vehicle combinations with composite material pressure vessels can transport more gas than steel pressure vessels. The technical characteristics of pressure vessels (material, volume, and pressure) directly affect the total vehicle mass, influencing fuel consumption.
- Vehicle combinations with composite pressure vessels achieve better vehicle mass utilization, reducing operational costs.

2. Methodology

The model shown in fig. 1, was designed to assess the fuel consumption of vehicle combinations intended to transport CNG (class 2 dangerous goods). Model input parameters, variables, and equations applied in the procedure are detailed in tab. 7, Appendix A.

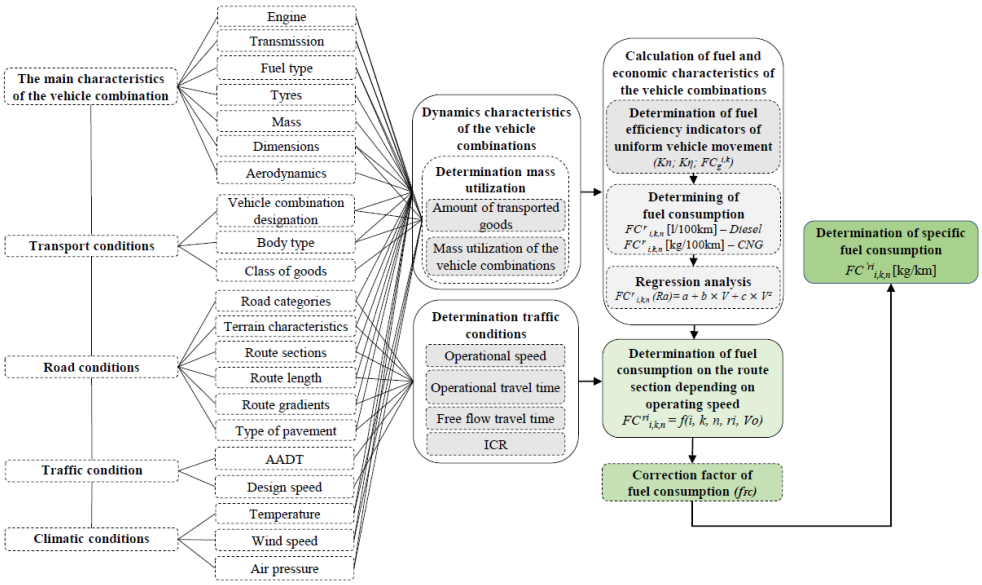

Figure 1. Model for predicting fuel consumption

In the first step of the procedure, the input parameters necessary for the model's functioning are defined. These input parameters include data on the main technical characteristics of the vehicles and bodies under consideration and operating, transport, travel, traffic, and climatic conditions. Parameters describing the technical characteristics of the considered vehicle combinations include information on engines and power transmission systems, fuel types, gearboxes, main power transmissions, and dimensional, mass, and aerodynamic characteristics. Transport conditions include the vehicle combination designation, body types, and class of goods. Road conditions include road categories and classifications (e.g., motorway, urban road, rural road), terrain characteristics, number

and length of route sections, number of longitudinal ascents and descents, and road pavement condition.

The traffic conditions on the route *(r)*, i.e., the route section *(r_i)*, are defined by the average annual daily traffic *(AADT)*, the designed speed *(V_d)*, the number of traffic lanes, and the capacity of the route section. Determination of the parameters that define road and transport conditions for the considered *r* was performed for all r_i, their lengths *(L_{ri})*, and longitudinal slopes *(u_{ri})* on the total length of the route *(L_r)*. The values of u_{ri} were determined by data referring to the terrain configuration on *r* or r_i located and data on the average elevations of the longitudinal profile of the road [19]. Climatic conditions are identified as average values of temperature *(t)*, wind speed *(V_w)*, and air pressure *(p_a)*, which correspond to the regional area where the roads are located [20].

In the second step, the dynamic characteristics of vehicle combinations were determined according to the laws of vehicle dynamics. Additionally, it thoroughly defined the parameters that characterize the traffic conditions on the selected route. The analysis was performed for vehicle combinations with different variants of subsystems (primarily fuel type and body type) based on the previously mentioned input parameters and data on transported gas amounts and vehicle mass utilization. The input parameters of engines correspond to the external speed characteristic. Data on the considered engines in operation were taken from the databases of vehicle manufacturers [21, 22]. By applying the known data on the speed characteristics of the engine and the power transmission system, traction and power balances were determined for each gear ratio. The values of the forces and resistance to motion acting on the vehicle combination depend on the type of vehicle combination *(i)*, body type *(n)*, fuel type *(k)*, and route *r*, i.e., route section r_i. By applying the formulas listed in tab. 7, the values of forces and resistance (circumferential force *($F_o^{i,n,k,r}$)*, drag resistance *($R_d^{i,n,k,r}$)*, grade resistance *($R_g^{i,n,k,r}$)*, rolling resistance *($R_f^{i,n,k,r}$)*, transmission resistance *($R_{tr}^{i,n,k,r}$)*, trailer resistance *($R_t^{i,n,r}$)*, vehicle weight *($G^{i,n,r}$)*, reactions in contact between the wheel and the surface). Following the analysis of the dynamic characteristics, parameters defining the traffic conditions (operational travel time *(t_o)*, free flow travel time *(t_f)*, operational speed *(V_o)*, and flow and capacity ratio *(ICR)*) were determined for the selected route. The values of t_o and V_o for each route *r*, i.e., route section r_i, were calculated using the flow and capacity ratio *ICR*, applying the formulas listed in tab. 7 [23, 24].

In the third step of the procedure, the Schlippe method was used to determine the specific fuel consumption *($FC_g^{i,k}$)*. This method involves calculating the coefficients K_n and K_η, which depend on the engine type and fuel type *k* (tab. 7) [25, 26]. The coefficient K_n considered the change in the specific effective fuel consumption *($FC_e^{i,k}$)* at the maximum effective engine power *(P_{emax})* from the change in the number of engine speeds *(n_e)*. The values of K_n are determined using formula (2), specified in tab. 7, correspond to the average values for the working cycles of Otto and Diesel engines. The initial values of $FC_e^{i,k}$ correspond to the fuel consumption at the maximum effective power of the engine P_{emax} and are determined according to data [21, 22]. The coefficient K_η considers the change engine efficiency *(K_p)* and its values are determined using formula (3) and correspond to average values for Otto and Diesel operating cycles with direct injection. Applying the specific values (K_η and K_n) and formula (4), the specific fuel consumption $FC_g^{i,k}$ was determined for each gear ratio *(N)* and the full range of n_e. Fuel density *(ρ_k)* depends on the type of fuel *k*, and its values are for natural gas (NG) $\rho_{NG} = 0.71$ [kg/m^3], i.e., for diesel fuel $\rho_{diesel} = 0.835$ [kg/l] [27, 28].

According to previously determined values ($R_d^{i,n,k,r}$, $R_g^{i,n,k,r}$, $R_f^{i,n,k,r}$, $R_{tr}^{i,n,k,r}$, $R_t^{i,n,r}$, K_n, K_η, $FC_e^{i,k}$, ρ_k, η_p) using formula (1) [25], fuel consumption *($FC^{r}_{i,k,n}$)* was determined for the considered combinations of vehicles.

$$FC^{r}_{i,k,n} = \frac{K_n \times K_\eta \times FC^{i,k}_e}{\eta_p \times \rho_k \times 36 \times 10^3} \times \left(\frac{c^{i,n}_x \times \rho_v}{2} \times A^{i,n} \times \left(V \pm V_w\right)^2 + G^{i,n,k} \times \cos\alpha \times f^{r}_u \pm G^{i,n,k} \times \sin\alpha \right) \quad (1)$$

The $FC^{i,k,n}_r$ values are expressed in kilograms of fuel burned per 100 kilometers traveled for CNG-powered vehicles, i.e., in liters per 100 kilometers traveled for diesel-powered vehicles. After determining specific values of $FC^{i,k,n}_r$, the functional dependence on $FC^{i,k,n}_r$ of the vehicle

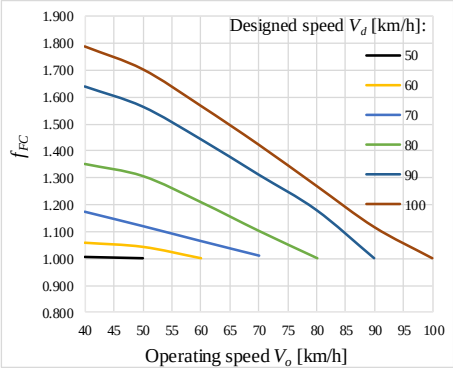

Figure 2. Dependence of the fuel consumption correction factor on the change speed from V_d to V_o

combination speed for each gear *(N)* in the gearbox, the fuel economy curve, was determined by applying regression analysis *(R_a)*. The functional dependence of $FC_r^{i,k,n}$ *(R_a)* is determined using the formula (5). Formula (5) is a polynomial of the second degree determined by the regression parameters represented by the labels *a*, *b*, and *c* listed in tab 7. Using previously determined data, the resulting consumption curves for individual gear ratios in the gearbox $FC_r^{i,k,n}$ *(Ra)* and operational speeds V_o on the route, in the fourth step, the fuel consumption $FC_{i,k,n}^{ri}$ was determined based on a second-degree polynomial obtained through regression analysis for each r_i depending on V_o. In the fifth step of the procedure, $FC'_{i,k,n}^{ri}$ values were determined and corrected by applying the fuel consumption correction factor *(f_{FC})*. The correction factor f_{FC} includes the increase in fuel consumption caused by the mutual influence of vehicles in the traffic flow, i.e., the change in vehicle speed from V_d to V_o [29], as shown in fig. 2. The speed change values (V_d to V_o) shown in fig. 2 were determined by regression analysis of data from the matrix of correction factors obtained from the literature [29].

2.1. Parameters that describe the technical characteristics of vehicles and bodies

The research subject includes trucks, trailers, and bodies intended for CNG transport. tab. 1, and tab. 2, show the input parameters necessary for the model's functioning. The mentioned parameters describe the technical characteristics of vehicles, tractors (BC) in category N_3, and semi-trailers (ST) in category O_4. tab. 1, lists the input parameters of considered BCs on fuel type, axle configuration, tires, mass characteristics, engines, and power transmission systems.

Table 1. Parameters describing the technical characteristics of considered BC

Vehicle:	Unit	Tractor (BC)[1]	Tractor (BC)[2]
Fuel type *k*:	[-]	CNG	Diesel
Axle configuration:	[-]	4×2	4×2
Tyres:	[-]	315/70 R 22.5	315/70 R 22.5
Tractor mass in running order with *k* (M_s^k):	[kg]	8119	7700
Number of gears *(N)* and gearbox type:	[-]	12–automatic	12–automatic
Final drive ratio (i_o):	[-]	3.36	2.41
External (speed) characteristics of the engine			
Specific effective fuel consumption ($FC_e^{i,k}$):	[g/kWh]	227	187
Maximum engine torque (M_{emax}):	[Nm]	2000	2100
Engine speed at maximum torque (n_{Memax}):	[rpm]	1100	1100
Maximum engine power (P_{emax}):	[kW]	338	310
Engine speed at maximum engine power (n_{Pemax}):	[rpm]	1900	1600

[1] *https://bb-portal.mercedes-benz-truck.com/-tehnical data - specification*
[2] *https://newibb.iveco.com/ - tehnical specification*

The values of the transmission efficiency coefficient *(η_p)* were determined using the formula (6) specified in the tab. 7. The values of η_p correspond to the concept with longitudinally placed transmission elements and a rear-axle drive. The efficiency coefficients for the transmission elements, coupling *(η_{ps})*, gearbox *(η_{pm})*, propeller shaft *(η_{pzp})*, differential *(η_{pgp})*, and driveshaft *(η_{ppv})*, were determined using the provided data [30, 31]. The static radius value of the wheel *(rs)* was determined based on the tire data mentioned in the tab. 1, and using the formula (7), tab.7. Parameters: wheel rim diameter *(R)*, tire deformability coefficient *(λ)*, and nominal ratio *(K)*, which represents the ratio of tire profile height *(h)* and tire width *(w)*, were determined by data [21, 22, 32].
Tab. 2, presents the input parameters describing the considered semi-trailers. Depending on the body type *n*, type of pressure vessel, tire dimensions, mass characteristics, total volume, and permissible working pressure are provided. The semi-trailers are equipped with devices and equipment on their cargo areas to accommodate battery or MEGC bodies, featuring two types of pressure vessels: Type–1 and Type–4 [33].

Table 2. Parameters describing the technical characteristics of considered ST

Vehicle:	Unit	Semi-trailer (ST)	Semi-trailer (ST)
Body types *n*:	[-]	Battery	MEGC
Types of pressure vessels:	[-]	Type–1	Type–4
Material of pressure vessels:	[-]	Steel	Composite
The number of axles and wheels:	[-]	3/6	3/6
Tyres:	[-]	385/65 R22.5	385/65 R22.5
Trailer mass in running order with *n* (M_{st}^{n}):	[kg]	28340	22160
Payload capacity with *n* ($M_n^{i,n}$):	[kg]	6660	12840
Reduced vehicle payload capacity ($M_{rn}^{i,n}$):	[kg]	5541	11721
Total volume of vessels ($V^{i,n}$):	[dm^3]	22350	39900
Permissible working pressure of the vessels ($P^{i,n}$):	[MPa]	20	25

The model includes the influences of the mass characteristics of the considered combinations concerning the legal restrictions regarding the total permissible mass of the vehicle combinations on the roads by introducing reduced vehicle payload capacity ($M_{rn}^{i,n}$). It introduces the dependence of transported quantities of gas on the technical characteristics of the vehicle and body type, the influence of the chemical characteristics of the gas, and temperature conditions during filling, shown in tab. 7 formula (8). Reduced vehicle payload capacity ($M_{rn}^{i,n}$) agrees with technical restrictions regarding the maximum permissible mass of vehicle combinations, as defined in Regulation [34].

2.2. Transport conditions

The model identifies the effects of transport conditions on fuel consumption depending on vehicle combination designation, class of dangerous goods (CNG), body type, and amount of transported goods. The analysis includes the vehicle combinations (1, 2, 3, and 4), BC with diesel and CNG drive, and ST with Type–1 and Type–4 bodies, specified in tab. 1, and tab. 2. Considered vehicle combinations:

- $(BC)_D$ + (ST) Type–4: BC powered with diesel and ST with MEGC body and Type–4 vessels (vehicle combination 1),
- $(BC)_D$ + (ST) Type–1: BC powered with diesel and ST with battery body and Type–1 vessels (vehicle combination 2),
- $(BC)_{CNG}$ + (ST) Type–4: BC powered with CNG and ST with MEGC body and Type–4 vessels (vehicle combination 3),
- $(BC)_{CNG}$ + (ST) Type–1: BC powered with CNG and ST with battery body and Type–1 vessels (vehicle combination 4).

The amount of transported gas $M_t^{i,n}$ and the vehicle's mass utilization depend on the vehicle combination *i*, body type *n*, and fuel type *k*. The model considers the influences from *i*, *n*, and *k* on increasing the combination's total mass ($M_{vc}^{i,n,k}$) and $M_t^{i,n}$. The quantity $M_t^{i,n}$ is directly dependent on the *i*, *n*, and chemical characteristics of the gas; its values are determined by applying the formula (8) specified in tab. 7. To simulate the working conditions during the filling of vessels, the model includes input parameters resulting from climatic conditions and technical characteristics of the considered bodies on the filling of pressure vessels and $M_t^{i,n}$. The included input parameters are *t*, total vessel volume ($V^{i,n}$), vessel

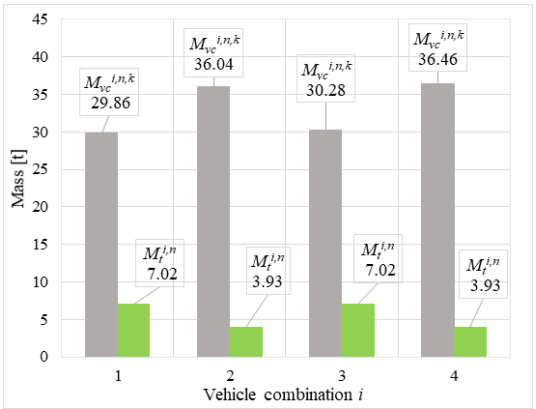

Figure 3. Mass characteristics of the analyzed vehicle combinations

operating pressure ($P^{i,n}$), molar masses of gas (m_g), and compressibility factor (Z). The Z factor is a variable and depends on the working pressure and temperature [35]. The values of factor Z for NG were determined based on the input parameters t [20] and $P^{i,n}$ of the considered bodies, as shown in tab. 3. The adopted values of the factor Z = 0.798 correspond to the conditions (t = 15 °C i $P^{i,n}$ = 20 MPa). The m_g values were determined based on the data [27]. The effects of n i k on increasing the total masses of the combinations $M_{vc}^{i,n,k}$, and $M_t^{i,n}$ are shown in fig. 3, where the stated values of $M_t^{i,n}$ correspond to the conditions (t = 15 °C, $P^{i,n}$ = 20 MPa, ρ_{kNG} = 0.71 kg/m^3 and universal gas constants R_u = 8.314 J/molK). Fig. 3, shows the mass relations between the engaged mass capacities $M_{vc}^{i,n,k}$, and the amount of transported gas $M_t^{i,n}$ for the considered vehicle combinations (1, 2, 3, and 4). There are noticeable differences in the increase of $M_{vc}^{i,n,k}$ for vehicle combinations (2 and 4) with bodies Type–1 and CNG-powered compared to combinations (1 and 3) with diesel-powered and Type–4 bodies. The influence of the fuel type k on the increase of M_s^k at BC, and therefore $M_{vc}^{i,n,k}$, is noticeable in vehicles powered by CNG, i.e., combinations (3 and 4), shown in fig. 3. Namely, the additional installation of vehicles powered by CNG affects the increase of M_s^k at BC, and it is under the provisions related to special parts of the construction of motor vehicles powered by alternative fuels specified in the agreement [14]. The amounts of $M_t^{i,n}$ transported depend on the technical characteristics of the vessels, the temperature conditions during filling, and the chemical composition of the gas. Vehicle combinations (1 and 3) with body Type–4 transport, on average, 44% more gas than combinations (2 and 4) with Type–1 bodies. The effects of body type n on the vehicle's mass utilization and fuel consumption are noticeable for combinations with Type–1, and it depends on the material of the body's construction and the technical limitations of the pressure vessels ($V^{i,n}$ and $P^{i,n}$).

2.3. Road and traffic conditions

This chapter identifies road and traffic conditions that affect fuel consumption. The assessment model identifies the impact of road and traffic conditions on the change in V_o and resistance to motion, depending on the category of road and type of pavement structure and condition, number and length of road sections, and terrain characteristics (longitudinal slopes) the number of traffic lanes, and the capacity of the route section. For the model, an eight-kilometer route on road number 14, classified as a road category IB [19, 36], was chosen. This section is part of the Pančevo-Kovin route and was arbitrarily selected as a representative straight-road segment. The route has two lanes in both directions and is divided into eight sections with a length of one kilometer. The average u_{ri} values for each r_i were determined as the mean slope values based on the data on the change in elevation of the longitudinal road profiles [19] shown in fig. 4. The values of the grade resistance $R_g^{i,n,k,r}$ are dependent on u_{ri}, and have a positive sign (+) for ascents and (–) for descent, determined by applying formula (9), tab. 7. Traffic conditions on the considered section include input parameters, the number of traffic lanes, the capacity of the route section, V_d, and $AADT$, based on which the values of (V_o, t_f, and t_o) were determined for each r_i. Data on $AADT$ by vehicle category were taken from the database [36]. The traffic sign determines the values of V_d for the selected route sections. The t_o values tab. 4., were determined by applying the Bureau of Public Roads (BPR) formula (10), listed in tab. 7.

Table 3. Parameters describing the road and traffic conditions

Sections of road r_i	Mean elevation value [m]	Free flow travel time t_f [h]	Operational travel time t_o [h]
r_{1-2}	76.091	0.020	0.027
r_{2-3}	76.780	0.025	0.034
r_{3-4}	76.243	0.017	0.023
r_{4-5}	76.653	0.017	0.023
r_{5-6}	76.313	0.017	0.023
r_{6-7}	76.319	0.013	0.017
r_{7-8}	77.454	0.013	0.017
r_{8-9}	76.511	0.013	0.017

Formula (10) shows the dependence t_o of this as a function of travel time in free flow (t_f), ICR, and correction coefficients α and β. Values t_f tab. 4., are determined by the relation length of the road section L_{ri} divided by the design speed V_d. The ICR of a road section is the actual flow (q) divided by the maximum volume of traffic that can flow through a road section (capacity of the road section) [23]. The values of the coefficients α and β depend on the category and classification of the road, and

the values α = 0.5 and β = 2.5 were adopted for the considered route r [23]. Based on previously determined values, using formula (11) listed in tab. 7, V_o was determined for each r_i [37]. The initial values of the rolling resistance coefficient (f_o^r) correspond to the data on the road category and the condition of the road infrastructure. For the model, an initial value of f_o^r =0.006 was adopted, corresponding to the data for truck tires and asphalt pavement [38]. The values of the total coefficient of rolling resistance $(f_u{}^r)$ are determined by applying formula (12) [32].

2.4. Climatic conditions

The developed model identifies the effects of climatic conditions (average values of t, V_w, and p_a) on changes in $M_t^{i,n}$, $M_{vc}^{i,n,k}$, and resistances to motion. The input parameters required for the model's functioning (t, V_w, and p_a) are determined based on the database [20] and correspond to the regional area of the route section. Values of $R_d^{i,n,k,r}$ depending on the angle of wind direction, formula (13) shown in tab. 7. If the direction of action V_w is in the direction of vehicle combinations speed, then the speed has a positive sign (+), that is (–) for action in the opposite direction. The model processes only the effects of wind speed in the longitudinal direction of the vehicle combination. The air density values (ρ_v), which affect $R_d^{i,n,k,r}$, were determined using the formula (14) shown in tab. 8. The model identified the effects of temperature t on $M_t^{i,n}$ and $M_{vc}^{i,n,k}$ and resistances to motion. The dependence of $M_t^{i,n}$ on t was determined using the formula (8) shown in tab. 7.

3. Results and discussion

This chapter presents the results of the fuel consumption estimation model, demonstrating the impact of pivotal parameters on the fuel economy of the analyzed vehicle combinations. The model combines the technical characteristics of the vehicles with various operating conditions, displaying the results as fuel consumption expressed in kilograms of fuel burned per kilometer traveled. The model results are shown in fig. 4, 5, and 6. Changes in the vehicle combinations speed, caused by the mutual influence of vehicles in the traffic flow, and changes in the longitudinal slopes u_{ri} resulting from elevation changes along route sections r_i over the entire length of the considered route r, are illustrated In fig. 4. This illustration provides a detailed overview of the speed changes (V_d to V_o) due to the interaction between vehicles on different route sections.

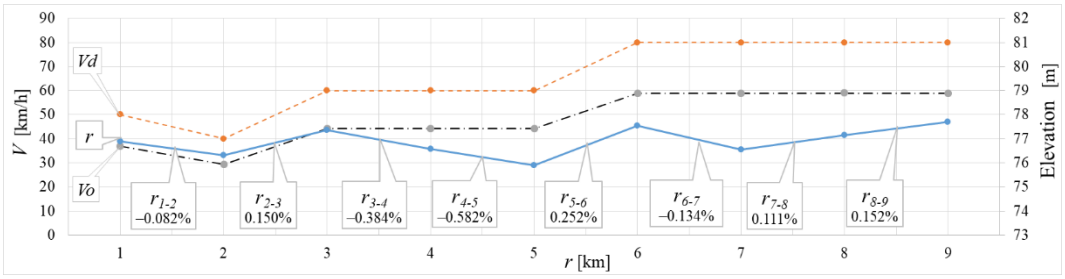

Figure 4. Changes in speed and grade on route *r*

The fuel consumption estimation model results for the considered vehicle combinations (1, 2, 3, and 4) are presented in fig. 5 and 6, covering the route sections r_i along the entire length of the considered route r. The results shown correspond to the loaded vehicles mode and represent the dependence of the average fuel consumption on the change in V_o on each route section r_i. Fig. 5 shows fuel consumption $FC'^{ri}_{i,k,n}$ for combinations (1 and 2) powered by diesel fuel. Combination (2) with a Type–1 body for the same road conditions (V_o and u_{ri}) has, on average, 6.2% higher fuel consumption than combination (1) with a Type–4 body. The influence of body type n on the increase of the total mass of the combination $M_{vc}^{i,n,k}$ of the transported amount of gas $M_t^{i,n}$, shown in Chapter 3.2 on fig. 3,

is also noticeable in the increase of $FC'^{ri}_{i,k,n}$. This difference in fuel consumption highlights the impact of body type on overall fuel consumption for identical operating conditions.

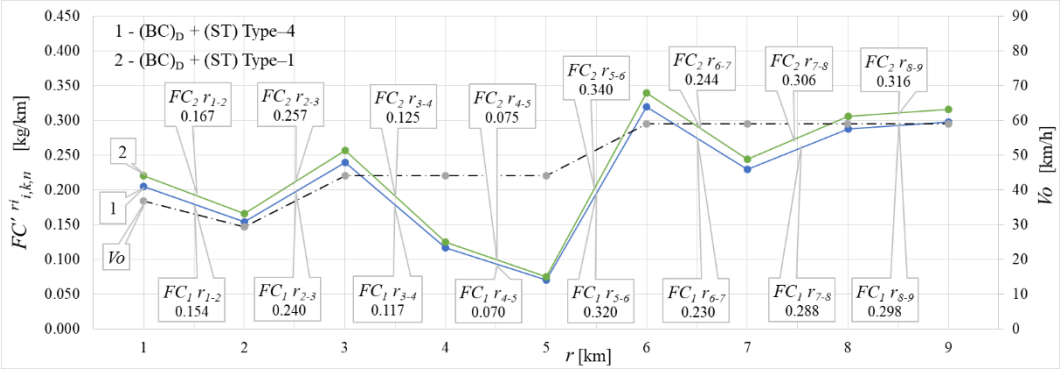

Figure 5. Estimated fuel consumption for the diesel-powered vehicle combinations 1 and 2 on route *r*

In the second case, fig. 6, shows the $FC'^{ri}_{j,k,n}$ fuel consumption for combinations (3 and 4) powered by CNG fuel. The results show a similar situation to the previous case; for the same road conditions, combination (4) with a Type–1 body has 6.1% higher consumption on average than combination (3) with a Type–4 body.

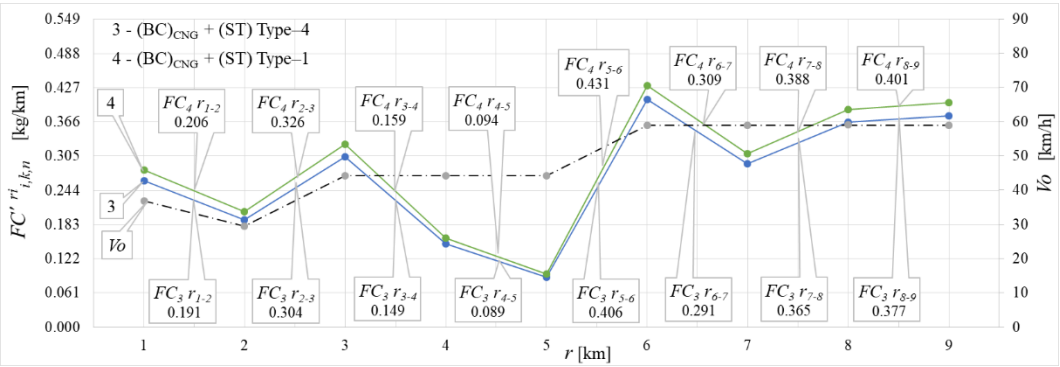

Figure 6. Estimated fuel consumption for the CNG-powered vehicle combinations 3 and on route *r*

The differences in fuel consumption obtained by the model for the considered vehicle combinations are caused by input parameters, primarily the specific effective fuel consumption $FC_e^{i,k}$, and mass characteristics of the vehicle, shown in Chapter 3.2.

3.1. Fuel costs analysis

Since this paper analyzes the fuel consumption of transport vehicles that differ in tractor fuel and the amount of natural gas transported, comparing four alternatives requires introducing costs into the analysis. In this regard, in tab. 4, and based on data on average fuel consumption from fig. 5 and fig. 6 and previously calculated prices for one kilogram of fuel (2.02 EUR/kg diesel and 1.03 EUR/kg CNG), the fuel costs per kilometer were calculated and presented.

Table 4. Fuel costs per kilometer for different vehicle combinations [EUR/km]

No.	Vehicle combinations	r_{1-2}	r_{2-3}	r_{3-4}	r_{4-5}	r_{5-6}	r_{6-7}	r_{7-8}	r_{8-9}
1	BC_D + (ST) Type–4	0.337	0.521	0.254	0.152	0.771	0.554	0.694	0.705
2	BC_D + (ST) Type–1	0.313	0.486	0.238	0.143	0.725	0.520	0.653	0.663
3	BC_{CNG} + (ST) Type–4	0.211	0.334	0.163	0.097	0.494	0.355	0.445	0.462
4	BC_{CNG} + (ST) Type–1	0.196	0.312	0.152	0.091	0.465	0.334	0.418	0.435

The costs were calculated for both fuel (diesel and CNG) and all observed route sections. It should be emphasized that the calculated costs depend on current market prices of energy sources. These calculated costs highlight CNG vehicles' more favorable fuel cost efficiency compared to comparable diesel vehicles. However, to get a clearer picture, it is necessary to consider the amount of CNG transported, which allows us to calculate the average costs per ton-kilometer for each analyzed vehicle combination. These costs are presented in tab. 5.

Table 5. Fuel costs per kilometer, per ton of transported gas for different vehicle combinations [EUR/tkm]

No.	Vehicle combinations	r_{1-2}	r_{2-3}	r_{3-4}	r_{4-5}	r_{5-6}	r_{6-7}	r_{7-8}	r_{8-9}
1	BC_D + (ST) Type–4	0.048	0.074	0.036	0.022	0.110	0.079	0.099	0.100
2	BC_D + (ST) Type–1	0.080	0.124	0.061	0.036	0.184	0.132	0.166	0.169
3	BC_{CNG} + (ST) Type–4	0.030	0.048	0.023	0.014	0.070	0.051	0.063	0.066
4	BC_{CNG} + (ST) Type–1	0.050	0.079	0.039	0.023	0.118	0.085	0.106	0.111

The calculated average costs reveal that, of the four considered alternatives, the lowest average costs in gas transportation, on all observed sections, are achieved by vehicle combinations whose tractors use CNG as fuel and which use semi-trailers with Type–4 vessels to perform their primary activity. In this case, the specified combinations range from 0.014 to 0.070 EUR per tkm. Otherwise, it is noticeable that these costs vary significantly along the route, i.e., by section. Fuel costs are 36% lower on average for vehicles powered by CNG and semi-trailers with Type–4. This applies to all four analyses of vehicle combinations. Given the above, quite expectedly, these vehicle combinations achieve the lowest total fuel costs in gas transportation on the entire route. Therefore, gas transportation with this type of transport is considered the most efficient, at least in terms of fuel costs. On the other hand, the highest average fuel costs are recorded by vehicle combinations that use diesel as a fuel and transport a smaller amount of gas (semi-trailers with vessels Type–1). What is particularly interesting is that the two remaining vehicle combinations, which differ in both considered parameters, record approximately the same amount of costs. However, these costs are lower in the vehicle combinations that use CNG fuel.

3.2. Model validation

Validation of the model was performed on the results of fuel consumption *(FC)* monitoring of the observed vehicle combinations using onboard diagnostics (OBD) on the road, which also includes the considered route sections [33]. These data enabled a comparison with the model's estimates, establishing its accuracy and reliability in estimating fuel consumption. Model deviation results - deviations between monitored *FC* fuel consumption values and fuel consumption values determined by the model $FC'^{ri}_{i,k,n}$ for each route section r_i are displayed using two metrics: absolute error (AE) and relative error (RE). The model's accuracy was evaluated with two statistical measures: mean absolute error (MAE) and mean absolute percentage error (MAPE), with the values for each vehicle combination shown in tab. 6.

Table 6. Comparison of performance of the model

No	Vehicle combinations	AE and RE values per road sections									MAE	MAPE
			r_{1-2}	r_{2-3}	r_{3-4}	r_{4-5}	r_{5-6}	r_{6-7}	r_{7-8}	r_{8-9}	[kg/km]	[%]
1	BC_D + (ST) Type–4	AE [kg/km]	0.010	0.015	0.007	0.005	0.019	0.014	0.020	0.018	0.014	5.965
		RE [%]	5.810	5.808	5.797	6.579	5.605	5.815	6.494	5.815		
2	BC_D + (ST) Type–1	AE [kg/km]	0.007	0.012	0.005	0.004	0.015	0.015	0.011	0.016	0.011	4.465
		RE [%]	4.298	4.283	3.932	5.305	4.226	5.644	3.342	4.692		
3	BC_{CNG} + (ST) Type–4	AE [kg/km]	0.018	0.033	0.016	0.008	0.040	0.023	0.041	0.035	0.027	8.926
		RE [%]	8.743	9.725	9.889	8.164	9.026	7.328	10.072	8.462		
4	BC_{CNG} + (ST) Type–1	AE [kg/km]	0.033	0.048	0.024	0.014	0.062	0.046	0.059	0.060	0.043	13.044
		RE [%]	13.981	12.917	13.220	12.538	12.610	12.832	13.186	13.071		

By comparing the model results with fuel consumption data from a previous study [33], significant matches were observed, especially concerning the increased fuel consumption of vehicle combinations with Type–1 vessels. This increase in consumption is particularly pronounced for CNG-powered combinations with Type–1 vessels. The results show that the model accurately predicts the increase in fuel consumption of the combination, considering all the parameters resulting from the operation conditions described in the previous chapters. The lowest model error was observed for diesel-powered vehicle combinations with Type–1 bodies, with the highest average gas transport costs. On the other hand, the largest model errors were observed for CNG-powered combinations. CNG-powered vehicles have higher fuel consumption due to specific effective fuel consumption parameters and the physical and chemical differences between CNG and diesel. These differences for stem from variations in fuel composition (CNG), which can vary depending on the fuel distributor, affecting combustion efficiency and overall fuel consumption. The input parameters describing the technical characteristics of the vehicles used in the model, as outlined in Chapter 3.1, are consistent with the vehicle characteristics from the research [33].

3.3. Comparative Review of Existing Research

The review of previous research covered the main aspects, focusing on model development and analysis to gain insight into current methodological approaches and findings in this field. This review examined the concepts and fundamental principles used in existing models, the work activities and specific tasks of HDVs, and the primary input parameters needed to operate the model. Model deviations were also considered, i.e., differences between predicted and actual values. Finally, the similarities and differences between the existing models and the new model proposed in this paper were compared to highlight the new model's improvements and innovations.

Barth et al. [1], Edwardes et al. [2], and Peng et al. [3] developed models to estimate fuel consumption and exhaust emissions for trucks and buses based on vehicle and engine specifications and operating conditions, with errors between 5% and 25%. The proposed model in the paper also considers the input parameters resulting from the technical characteristics of the vehicle and engine, as well as the parameters describing transport, road, climate, additionally evaluating, and traffic conditions. The considered models do not include changes in fuel consumption concerning traffic conditions on the route or the specifics of vehicles intended to transport gases. Primary changes in fuel consumption and transported goods (gas) quantities depend on operational conditions. Research [4] and [5] developed comprehensive models to estimate exhaust emissions and fuel consumption for various vehicle categories, including heavy vehicles. These models use statistical data based on vehicle and engine technical characteristics and include part of the operating conditions, aiming to predict annual fuel consumption for tactical and strategic management. The basic similarities with the model presented in the paper are in the input parameters that refer to part of the operational and technical characteristics of the vehicle and the engine. While these models share input parameters related to vehicle and engine operations with the model presented in this paper, they do not account for the specifics of gas-transport vehicles or the impact of traffic flow on operating speed. Dindarloo and Siami-Irdemoosa [6] developed a fuel consumption model for heavy dump trucks in mines based on

vehicle mass utilization and the time spent on loading, transporting, and unloading activities. The model has an error rate of around 6% and accounts for vehicle mass and the amount of goods transported. However, it does not consider the specifics of gas-transport vehicles or the mutual influence of vehicles in the traffic flow on operating speed. The developed model presented in the paper also considers the mass utilization of vehicles and the amount of goods transported. Alamdari S. et al. [7] use many input parameters, which derive from the vehicle's technical characteristics and operational conditions, including transport, road, climatic conditions, fleet management, and operator influences. Pereira, G. et al. [8] and Katreddi, S. et al. [9], in their models, focus on vehicle mass utilization, road construction, road length, and slope, i.e., on engine characteristics and vehicle speed. The error values of the considered models range from 1% to 21%. Gong et al. [10] present a model that focuses on the effects of the technical characteristics of the vehicle and engine, as well as road and climate conditions, on the fuel consumption of trucks. The error values of the model depend on the applied decision algorithms and range from 13% to 18%. The similarities between the model in the paper and the mentioned models are primarily in the input parameters that cover the technical characteristics of the vehicle and the considered engines, as well as the influences resulting from the vehicle's operating conditions. However, the existing models do not account for the specifics of gas-transport vehicles. Perrotta et al. [11] developed fuel consumption estimation models that incorporate input parameters such as total vehicle mass, road gradients, route characteristics, torque dependence on transmission gear, vehicle speed, and acceleration, achieving error rates of around 3%. Fang et al. [13] and Kan et al. [14] also presented fuel consumption models for HDVs based on deep learning techniques, specifically artificial neural networks, which process engine characteristic data. These models have error rates ranging from 5% to 14%. However, Ivković et al. [37] introduced a model for estimating fuel consumption, exhaust emissions, and emission costs across different vehicle categories. This model primarily estimates emissions of Carbon Dioxide (CO_2), Methane (CH_4), and Nitrous Oxide (N_2 O) by calculating fuel consumption using the Highway Development and Management Model (HDM) while considering traffic conditions. Including detailed parameters on traffic and road conditions enhances the model's accuracy and applicability in estimating fuel consumption and gas emissions. Similar to the model presented in this paper, model [37] analyzes the impact of traffic and road conditions on fuel consumption and emissions.

The primary difference between the model presented in this paper and previous models is its specific application for vehicles intended for CNG transportation. It incorporates various body types and technical parameters (working volume, pressure, construction materials, gas chemical properties, and filling temperature). These parameters significantly influence the amount of gas transported, vehicle mass utilization, fuel consumption, and fuel costs. By integrating these specific parameters, the model provides a more accurate assessment of fuel consumption and total fuel costs for CNG transportation. The proposed model's contribution is to provide data on potential fuel consumption and fuel costs for vehicles intended for CNG transportation, which is a primary criterion for selecting new vehicles and bodies. The developed model can also be applied to existing vehicle fleets with the same activity that strives to improve productivity, primarily through pressure vessels made of composite materials and alternative fuels for vehicle propulsion.

3.4. Limitations of the model and future research

The model has limitations: it estimates fuel consumption under idealized conditions with constant vehicle speed on longitudinal sections and assumes a constant road resistance coefficient. The rolling resistance coefficient is set based on vehicle type, pavement quality, and tire condition and remains constant across the entire road section. The model assumes professional drivers who consciously, safely, and economically operate vehicles. Predicting the impact of driver behavior is analytically challenging to determine, even during road tests, due to subjective factors affecting vehicle speed, engine operation, and vehicle management. However, with experienced and well-trained drivers, the negative impacts on safe and economical driving are significantly reduced. The

flexible model allows adaptation to different classes of dangerous goods within RTDG and other vehicle categories, thus expanding its applicability. This customization enables users to apply the model to various transport scenarios (vehicle categories), optimizing performance and meeting specific requirements for each type of goods or vehicle.
The model is an essential foundation for future research on the environmental impact of vehicles transporting dangerous goods, particularly regarding exhaust emissions, fuel consumption, and fuel costs. Developing the new model will provide fleet owners with additional data for selecting new vehicles and bodies. That will allow owners to choose vehicles that meet technical and operational requirements while optimizing them according to environmental and economic criteria, reducing emissions and operating costs and increasing fleet efficiency.

4. Conclusion

The paper introduces a model for estimating fuel consumption and fuel costs for vehicles transporting compressed natural gas, considering different fuel types (diesel or compressed natural gas) and body types. This model integrates the technical characteristics of vehicles and bodies with transport, road, climate, and traffic conditions to calculate average fuel consumption on specific route sections. It analyzes the fuel consumption of various vehicle combinations, including different semi-trailer bodies and the amount of gas transported in steel or composite pressure vessels. This analysis enhances understanding of how the vehicle body impacts fuel consumption and the volume of gas transported, aiding in optimizing consumption based on vehicle configuration and transport conditions. The presented model differs from previous models by specifically addressing CNG transportation and incorporating a wider range of technical parameters, enabling more accurate fuel consumption estimation and better fleet management decisions.
Model results show that vehicle combinations with steel pressure vessels consume more fuel than those with composite material vessels across all analyzed route sections. This increased consumption, averaging about 6%, occurs for diesel and compressed natural gas fuels. The higher fuel consumption in vehicles with steel pressure vessels is due to their greater mass. This additional weight requires the vehicle to expend more energy to overcome motion resistance, thereby increasing fuel consumption. These findings highlight the advantage of using composite materials to optimize fuel consumption and reduce fuel costs.
Vehicle combinations with pressure vessels made of composite materials can transport, on average, 44% more gas than those with steel vessels. This weight reduction allows for transporting additional pressure vessels, increasing the amount of gas carried without exceeding road safety limits on permissible vehicle mass. Vehicles with composite vessels utilize their capacity more efficiently, enabling them to transport more gas in a single trip, reduce the number of trips required, and lower overall transportation costs.
The analysis shows that the lowest fuel costs for gas transportation are achieved by vehicle combinations with CNG-powered tractors and semi-trailers using composite material pressure vessels. The calculated fuel costs presented in the paper are crucial for several reasons. They highlight potential savings from switching to more efficient vehicle combinations for natural gas transport. Additionally, they help evaluate whether these savings justify the higher initial costs of newer technological solutions when purchasing new vehicles. However, although fuel costs are a significant part of operating expenses, other cost factors must also be considered to make an informed decision.
The model's results correspond with monitoring the fuel consumption of the considered vehicle combinations realized in actual operational conditions. The proposed model provides fleet owners with data significant in decision-making procedures regarding selecting new vehicle combinations or converting existing ones to more modern ways of natural gas transportation to improve the fleet's efficiency.

.

Funding: This research was financially supported by the Ministry of Science, Technological Development, and Innovations of the Republic of Serbia (Contract No. 451-03-66/2024-03/200017, and No. TR36027).

5. Appendix A

Table 7. Appendix A explains the input parameters, variables, and formulas described in detail in the model.

Parameter – description		Unit	Acquisition	Ref.
i	Vehicle combination	[-]	The set of values related to the study area.	[-]
k	Fuel type	[-]	The set of values related to the vehicle(s).	[-]
n	Type of body	[-]	The set of values related to the vehicle(s).	[-]
r	Route	[-]	The set of values related to the study area.	[-]
r_i	Route section	[-]	The set of values related to the study area.	[-]
L_r	Total length of the route.	[m]	The set of values related to the study area.	[-]
L_{ri}	The length of the route section.	[m]	The set of values related to the study area.	[-]
V_d	The maximum design speed on the r_i route section.	[km/h]	The set of values related to the study area. Determined by a traffic sign.	[-]
u_{ri}	Longitudinal profile of road routes. Gradient of the r_i route section.	[%]	The set of values related to the study area. National databases.	[19]
f_o^r	The rolling resistance coefficient on the route r or r_i route section.	[-]	Pre-defined single value. Determined by the type of pavement construction.	[38]
$AADT$	Annual Average Daily Traffic on the route r.	[veh/day]	The set of values related to the study area.	[36]
t	Mean ambient temperature	[°C]	The set of values related to the study area.	[20]
p_a	Mean values of air pressure	[kPa]	The set of values related to the study area.	[20]
V_w	Mean wind speed	[m/s]	The set of values related to the study area.	[20]
	Vehicle characteristics			
M_s^k	Tractor mass in running order with k.	[kg]	The set of values related to the vehicle(s).	[21, 22]
M_{st}^n	Trailer mass in running order with n.	[kg]	The set of values related to the vehicle(s).	[33]
$M_{vc}^{i,n,k}$	The total mass of the vehicle combination i with n and k.	[kg]	The set of values related to the vehicle(s).	[21, 22, 33]
$M_n^{i,n}$	Payload capacity i with n.	[kg]	The set of values related to the vehicle(s).	[21, 22, 33]
A_f	Speed coefficient considers the influence of vehicle speed on the rolling resistance of the vehicle's wheels.	[-]	Pre-defined single value related to the study area.	[25]
$c_x^{i,n}$	Drag coefficient of the i with n.	[-]	Pre-defined single value related to the study area.	[25]
$A^{i,n}$	The frontal surface area of the i with n.	[m^2]	Pre-defined single value related to the vehicle(s). It was determined by measuring and planimetry of technical drawings of the considered vehicle.	[21, 22]
N	The number of gears in the gearbox of i depends on the engine type and k.	[-]	Pre-defined values related to the vehicle(s).	[21, 22]
i_m	The gearbox ratio of the i depends on the engine type and k.	[-]	Pre-defined values related to the vehicle(s).	[21, 22]
i_o	The final drive ratio of the i depends on engine type and k.	[-]	Pre-defined single value related to the vehicle(s).	[21, 22]
M_e	The effective engine torque of the i depends on engine type and k.	[Nm]	Pre-defined values related to the vehicle(s).	[21, 22]
P_e	The effective engine power of the i depends on engine type and k.	[kW]	Pre-defined values related to the vehicle(s).	[21, 22]
n_e	The engine speed of i depends on the engine type and k.	[rpm]	Pre-defined values related to the vehicle(s).	[21, 22]
$FC_e^{i,k}$	The specific effective fuel consumption at maximum engine power of the i depends on the engine type and k.	[g/kWh]	Pre-defined values related to the vehicle(s).	[21, 22]
K_p	The engine efficiency coefficient depends on the engine type (Otto or diesel working cycle) and k.	[-]	Determined values related to the engine types of the related vehicle(s).	[32]
ρ_k	Fuel density depends on k.	[kg/l] [kg/m³]	Pre-defined values related to the vehicle(s). The unit depends on the k for CNG [kg/m³] or diesel [kg/l].	[27, 28]
$V^{i,n}$	The total volume of pressure vessels of the i with n.	[dm^3]	The set of values related to the vehicle(s) and the study area.	[33]
$P^{i,n}$	Vessel working pressure depends on the n.	[MPa]	The set of values related to the study area.	[33]
m_g	Molar mass of gas	[g/mol]	The set of values related to the study area.	[27]
Z	The compressibility factor depends on the t and $P^{i,n}$.	[-]	The set of values related to the study area.	[35]
R_u	Universal gas constant	[J/molK]	Constant value 8.314	[35]
g	Gravitational acceleration	[m/s^2]	Constant value 9.81	[-]
The Algorithm Equations – description		**Unit**	**Equation – No**	**Eq. No**

K_n	The coefficient considers the effect of changes in engine speed on fuel consumption. The max. engine speed n_{Pemax} that corespond to P_{emax}.	[-]	$1.25 - 0.99\left(\frac{n_e}{n_{Pe\max}}\right) + 0.98\left(\frac{n_e}{n_{Pe\max}}\right)^2 - 0.24\left(\frac{n_e}{n_{Pe\max}}\right)^3$	(2)
K_η	The coefficient that takes into account changes in engine efficiency. The force (power) required to overcome the total grade P_g, rolling P_f, and drag resistance P_d.	[-]	$1.2 + 0.14\left(\frac{P_g + P_f + P_d}{\eta_p \times P_{emax}}\right) - 1{,}8\left(\frac{P_g + P_f + P_d}{\eta_p \times P_{emax}}\right)^2 + 1.46\left(\frac{P_g + P_f + P_d}{\eta_p \times P_{emax}}\right)^3$	(3)
$FC_g^{i,k}$	The specific effective fuel consumption of the i depends on the engine type and k.	[g/kWh]	$FC_e^{i,k} \times K_n \times K_\eta$	(4)
$FC^r_{i,k,n}(R_a)$	Fuel consumption of the i with n and k on the r determined by regression analysis.	[kg/100km] CNG or [l/100km] for diesel	$a + b \times V + c \times V^2$	(5)
η_p	Transmission efficiency coefficient of the i.	[-]	$\eta_p = \eta_{ps} \times \eta_{pm} \times \eta_{pap} \times \eta_{pgp} \times \eta_{ppv}$	(6)
r_s	The static radius of the wheel.	[m]	$0.5 \times R \times 0.0254 + K \times 10^{-2} \times w \times 10^{-3} \times \lambda$	(7)
$M_t^{i,n}$	The amount of gas transported. An active payload hauled by an i with an n.	[kg]	$\frac{m_g \times P^{i,n} \times V^{i,n}}{Z \times R_u \times (273.15 + t)}$	(8)
$R_g^{i,n,k,r}$	Total grade resistance force for i with n and k on the r.	[N]	$9.81 \times M_{vc}^{i,n,k} \times \sin\alpha$	(9)
t_o	Operational travel time depends on *AADT*, free flow travel time t_f, flow/capacity ratio *ICR*, and coefficients α and β on the r.	[-]	$t_f \times \left(1 + \alpha \times ICR^\beta\right)$	(10)
V_o	The operational speed on the r_i depends on operational time travel t_o and the length of the L_{ri}.	[km/h]	$\frac{L_{ri}}{t_o} = \frac{L_{ri}}{t_f \times \left(1 + \alpha \times ICR^\beta\right)}$	(11)
f_u^r	The total rolling resistance coefficient of the r is dependent on the vehicle speed.	[-]	$f_o^r \times (1 + A_f \times V^2)$	(12)
$R_d^{i,n,k,r}$	Total drag resistance force for i with n and k on the r.	[N]	$1.5 \times \frac{c_x^{i,n} \times \rho_v}{2} \times A^{i,n} \times \left(V \pm V_w\right)^2$	(13)
ρ_v	The air density depends on the t, p_a, and R_u.	[kg/m³]	$\frac{p_a}{R_u \times (273.15 + t)}$	(14)
$R_f^{i,n,k,r}$	The total rolling resistance force for i with n and k on the r.	[N]	$9.81 \times M_{vc}^{i,n,k} \times f^r \times \cos\alpha$	(15)
$R_{tr}^{i,n,k,r}$	Total transmission resistance for i with n and k on the r.	[N]	$\left(1 - \eta_p\right) \times P_e$	(16)
$R_t^{i,n,r}$	Total trailer resistance force for i with n on the r.	[N]	$9.81 \times (M_{st}^n \times f^r \times \cos\alpha + M_{st}^n \times \sin\alpha)$	(17)
$F_o^{i,n,k,r}$	Total circumferential force (traction force) on all driving wheels at uniform vehicle speed for i with n and k on the r.	[N]	$R_f^{i,n,k,r} + R_g^{i,n,k,r} \pm R_d^{i,n,k,r} + R_t^{i,n,r}$ $R_f^{i,n,k,r} - R_g^{i,n,k,r} \pm R_d^{i,n,k,r} + R_t^{i,n,r}$	(18)

Nomenclature

HDV – Heavy-Duty Vehicle
CNG – Compressed Natural Gas
RTDG – Road Transport Of Dangerous Goods
MEGC – Multiple Element Gas Containers
CMEM – Comprehensive Modal Emissions Model
VT-CPFM – Virginia Tech Comprehensive Power-Based Fuel Consumption Model
ECM – Engine-based Correction Model
MOVES – Motor Vehicle Emission Simulator
PLSR – Partial Least Squares Regression

ARIMA – Autoregressive Integrated Moving Average
RF – Random Forest
ANN – Artificial Neural Network
SVM –Support Vector Machine

GAN – Generative Adversarial Networks
MLP – Multi-Layer Perceptron
CE – Context Encoders
MF – Matrix Factorization
NG – Natural Gas
OBD – On-Board Diagnostics

MAE – Mean Absolute Error
MAPE – Mean Absolute Percentage Error
APMA – Algorithms Adaptive Polyploid Memetic Algorithm
CO_2 – Carbon Dioxide

CH_4 – Methan
N_2O – Nitrous Oxide
HDM – Highway Development and Management

Model

CNN – Convolutional Neural Network

6. References

[1] Barth, M., *et al*., Development of a heavy-duty diesel modal emissions and fuel consumption model, California Partners for Advanced Transportation Technology, UC Berkeley, USA, 2005

[2] Edwardes,W., *et al*., Virginia tech comprehensive power-based fuel consumption model, *Transportation Research Record, 2428(1)* (2014), pp. 1–9

[3] Peng, C., *et al*., Transient fuel consumption prediction for heavy-duty trucks using on-road measurements, *International Journal of Sustainable Transportation, 17(8)* (2023), pp. 956-967

[4] EPA, Environmental Protection Agency, Overview of EPA's MOtor Vehicle Emission Simulator (MOVES4), Washington D.C., USA, 2023

[5] Ankur, A. K., *et al*., A Versatile Model for Estimating the Fuel Consumption of a Wide Range of Transport Modes, *Energy, 15* (2022), 6, pp. 2232

[6] Dindarloo, S. R., *et al*., Determinants of fuel consumption in mining trucks, *Energy, 112* (2016), pp. 232-240

[7] Alamdari, S., *et al*., Application of machine learning techniques to predict haul truck fuel consumption in open-pit mines, *Journal of Mining and Environment, 13* (2022), 1, pp. 69-85

[8] Pereira, G., *et al*., Fuel consumption prediction for construction trucks: A noninvasive approach using dedicated sensors and machine learning, *Infrastructures, 6(11)* (2021), pp. 157

[9] Katreddi, S., *et al*., Trip based modeling of fuel consumption in modern heavy-duty vehicles using artificial intelligence, *Energies, 14(24)* (2021), pp. 8592

[10] Gong, J., *et al*., A comparative study on fuel consumption prediction methods of heavy-duty diesel trucks considering 21 influencing factors, *Energies, 14(23)* (2021), pp. 8106

[11] Perrotta, F., *et al*., Application of machine learning for fuel consumption modelling of trucks, *Proceedings* In 2017 IEEE International Conference on Big Data, Boston, USA, 2017, pp. 3810-3815

[12] Fang, C., *et al*., Fine-grained fuel consumption prediction, *Proceedings* of the 28th ACM International Conference on Information and Knowledge Management, New York, USA, 2019, pp. 2783-2791

[13] Kan, Y., *et al*., A deep learning engine power model for estimating the fuel consumption of heavy-duty trucks, *Proceedings* In 2020 6th IEEE International Energy Conference, Gammarth, Tunisia, 2020, pp. 182-187

[14] Economic Commission for Europe Inland Transport Committee, European Agreement Concerning the International Carriage of Dangerous Goods by Road (ECE/TRANS/326 Volumes I and II), United Nations, New York and Geneva, 2023

[15] Reddi, K., *et al*., Techno-economic analysis of conventional and advanced high-pressure tube trailer configurations for compressed hydrogen gas transportation and refueling, *International journal of hydrogen energy, 43(9)* (2018), pp. 4428-4438

[16] Mair, G. W., *et al*., Safety criteria for the transport of hydrogen in permanently mounted composite pressure vessels,*International Journal of Hydrogen Energy, 46(23)* (2021), pp. 12577-12593

[17] Solazzi, L., & Vaccari, M., Reliability design of a pressure vessel made of composite materials, *Composite structures, 279* (2022), pp. 114726

[18] Azeem, M., *et al*., Application of filament winding technology in composite pressure vessels and challenges: a review, *Journal of Energy Storage, 49* (2022), pp. 103468

[19] ***, Public Enterprise Roads of Serbia, Reference system, https://www.putevi-srbije.rs/referentni-sistem

[20] ***, Republic Hydrometeorological Institute of Serbia, https://www.hidmet.gov.rs

[21] ***, Mercedes Benz Truck Bodybuilder Portal, Tehnical data, https://bb-portal.mercedes-benz-truck.com/

[22] ***, Iveco Body Builder, Tehnical specification, https://newibb.iveco.com/
[23] Newton, S., Serbian National Transport Model System, Report No. R20090181/30670000/SNE/RLO, Zoetermeer, Netherlands, 2009
[24] Kuzović, L., *et al*., *Capacity of roads*, Construction book., Belgrade, Yugoslavia, 1989
[25] Selifonov, V. V., *et al*., *Theory of the vehicles*, Moscow State Mechanical Engineering University MAMI, Moscow, Russian Federation, 2007
[26] Kravets, V., *et al*., Technique for Determining the Fuel Consumption of a Vehicle on a Given Route, *Proceedings* of the 2nd International Conference on Modelling, Identification and Control (MIC 2015), Dordrecht, Netherlands, 2015, pp. 36-38
[27] ***, SERBIAGAS, Composition of natural gas, https://www.srbijagas.com
[28] Schaschke, C., *et al*., Density and viscosity measurement of diesel fuels at combined high pressure and elevated temperature, *Processes*, *1* (2013), pp. 30-48
[29] Kuzović, L., *Evaluation in the management of the development and exploitation of the road network*, University of Belgrade – Faculty of Transport and Traffic Engineering, Belgrade, Yugoslavia, 1994
[30] Litvinov, A. S., *et al*., *Theory of operational properties*, Mechanical Engineering, Moscow, Russian Federation, 1989
[31] Ivković, I., *Motor vehicles*, University of Belgrade – Faculty of Transport and Traffic Engineering, Belgrade, Serbia, 2020
[32] Khusainov, A., *Vehicle performance properties*, Ulyanovsk State Technical University ULSTU, Russian Federation, Ulyanovsk, 2011
[33] Vašalić, D., *et al*., Prediction of Fuel and Exhaust Emission Costs of Heavy-Duty Vehicles Intended for Gas Transportation, *Sustainability,16(13)* (2024), pp. 5407
[34] Ministry of Construction, Transport and Infrastructure of the Republic of Serbia, Regulation on the division of motor and trailer vehicles and technical conditions for vehicles in road traffic (No. 48/2023-101), Belgrade, Serbia, 2023
[35] GPSA, Gas Processors Suppliers Association, Engineering Data Book, twelfth (12th) ed., Tulsa, Oklahoma, USA, 2004
[36] ***, Public Enterprise Roads of Serbia, Traffic counting, https://www.putevi-srbije.rs/brojanje-saobraćaja
[37] Ivković, I., *et al*., The estimation of GHG emission costs in road and air transport sector: Case study of Serbia, *Transport, 33(1)* (2018), pp. 260-267
[38] Robert Bosch GmbH, Automotive Handbook, eleventh (11th) ed., USA, 2022

Submitted: 8.12.2024.
Revised: 15.02.2025.
Accepted: 21.02.2025.